HOSTED BY

ELSEVIER

CrossMark

Available online at www.sciencedirect.com

ScienceDirect

Progress in Natural Science: Materials International 25 (2015) 445–452

Progress in Natural Science Materials International

www.elsevier.com/locate/pnsmi
www.sciencedirect.com

Original Research

Wet spinning of PVA composite fibers with a large fraction of multi-walled carbon nanotubes

Dengpan Lai, Yizhe Wei, Liming Zou*, Yongjing Xu, Hongwei Lu

State Key Laboratory for Modification of Chemical Fibers and Polymer Materials, College of Materials Science and Engineering, Donghua University, 2999 North People Road, Shanghai 201620, China

Received 10 July 2015; accepted 16 August 2015
Available online 21 November 2015

Abstract

PVA composites fibers with a large fraction of multi-walled carbon nanotubes modified by both covalent and non-covalent functionalization were produced by a wet-spinning process. Model XQ-1 tensile tester, thermogravimetric analysis, scanning electron microscopy, differential scanning calorimetry, and wide-angle X-ray diffraction were used to characterize the properties of PVA/MWNT composite fibers. The TGA results suggested that MWNTs content in composite fibers were ranged from 5.3 wt% to 27.6 wt%. The mechanical properties of PVA/MWNT composite fibers were obviously superior to pure PVA fiber. The Young's modulus of composite fibers enhanced with increasing the content of MWNTs, and it rised gradually from 6.7 GPa for the pure PVA fiber to 12.8 GPa for the composite fibers with 27.6 wt% MWNTs. Meanwhile, the tensile strength increased gradually from 0.39 GPa for the pure PVA fiber to 0.74 GPa for the composite fibers with 14.4 wt% MWNTs. Nevertheless, the tensile strength of the composite fibers decreased as the MWNTs content up to 27.6 wt%. SEM results indicated that the MWNTs homogeneously dispersed in the composite fibers, however some agglomerates also existed when the content of MWNTs reached 27.6 wt%. DSC results proved strong interfacial interaction between MWNTs and PVA chain, which benefited composite fibers in the efficient stress-transfer. WXAD characterization showed that the orientation of PVA molecules declined from 94.1% to 90.9% with the increasing of MWNTs content. The good dispersibility of MWNTs throughout PVA matrix and efficient stress-transfer between MWNTs and PVA matrix may contributed to significant enhancement in the mechanical properties.

Keywords: Multi-walled carbon nanotubes (MWNTs); Poly (vinyl alcohol) (PVA); Wet-spinning; Composite fibers

1. Introduction

As organic polymers provide flexible molecular chain and inorganic matter possesses high modulus and high strength, composite materials with organic–inorganic components have excellent performance. Since the discovery in 1991 [1], carbon nanotubes have attracted a great deal of attention. In addition, carbon nanotubes are one of the most promising reinforcing inorganic matter in polymer matrix due to their excellent physicochemical properties. Solid progress has been made by previous studies by adding CNTs in polymer matrix to enhance mechanical [2] and electrical properties [3]. Among these composites, the fibers and yarns are the most promising forms for the application of individual CNTs on macroscopic materials because of the CNTs orientation along the fiber axis. However, there are some limitations in which CNTs aggregation in polymer matrix is the most serious problem. The reason is that CNTs lack functional groups and tend to aggregate with each other by virtue of strong van der Waals force resulting from high specific surface area [4]. Between agglomerates and polymer matrix, a number of voids/defects will generate and have an effect on the mechanical performance of composite fibers. Therefore, it is of great importance to avoid CNTs aggregation in polymer matrix. In previous studies, covalent [5,6] or non-covalent functionalization [7,8] has been adopted to improve the dispersibility of CNTs.

*Corresponding author. Tel.: +86 21 67792847; fax: +86 21 67792855.
E-mail address: lmzou@dhu.edu.cn (L. Zou).
Peer review under responsibility of Chinese Materials Research Society.

http://dx.doi.org/10.1016/j.pnsc.2015.10.003

In order to make the best of these excellent properties of individual CNTs, the loading of CNTs in the composites is expected to be increased as much as possible. Nevertheless, the mechanical test reveals that because of the formation of two-phase structure and void defects between CNTs and polymer [9], the mechanical property of composite fibers will decline as the loading of CNTs gradually increases to a high proportion (usually below 10 wt%). Therefore, it is more difficult to obtain high-performance composites containing high content of CNTs.

In general, melt-spinning and wet-spinning are involved in main spinning methods. Melt-spining is a common method to fabricate CNT/polymer composite fibers [10,11], however there are still some problems. As the content of CNTs reaches to a certain proportion, the viscosity of melt will increase shaply and makes CNTs disperse in polymer matrix unevenly, which will have an effect on melting polymer extrusion and fibers formation. On the contrary, wet-spinning has an advantage in fabricating composite fibers with high CNTs content [12]. The reason is that CNTs are dispersed in the polymer solution and the viscosity of spinning dope can be controlled through the addition of the solvent.

In this work, both non-covalent and covalent functionalization are employed to modify MWNTs. Covalent functionalization is adopted for introducing a number of oxygen-containing groups on the sidewall of MWNTs, while non-covalent functionalization is adopted by using PVA as the dispersant and matrix which could form strong interactions with MWNTs via hydrogen bond. By this means, MWNTs can be homogeneously dispersed in PVA matrix. It is well known that PVA possesses outstanding biocompatibility and water solubility [13]. At last, a range of PVA/MWNT fibers with high content of MWNTs were fabricated by wet spinning. It is noted that this PVA/MWNT composite fibers are also an enviroment-friendly material, for which H_2O is used as solvent. Model XQ-1 tensile tester, FT-IR, TGA, SEM, DSC, and WAXD were used to characterize modified MWNTs and PVA/MWNT composite fibers.

2. Experiment

2.1. Materials

The pristine MWNTs (Nanocyl™ NC7000 with the average diameter of 9.5 nm, length of 1.5 μm, carbon purity of 90% by TGA) were manufactured by a chemical vapor deposition (CVD) method, and purchased from Sambreville Nanocyl S.A (Belgium). PVA ($Mw \approx 114400$, 99% hydrolyzed) was received from Anhui Wanwei Updated High-tech Material Industry Co., Ltd. Concentrated sulfuric acid (98% H_2SO_4), concentrated nitric acid (65% HNO_3), methanol and ethanol were obtained from Sinopharm Chemical Reagent Co., Ltd.

2.2. Preparation of water-soluble PVA/MWNT spinning dope

After purified by heating and hydrochloric acid treatment, MWNTs were treated with strong mixed acid of concentrated H_2SO_4 (98%) and HNO_3 (65%) at a ratio of 3:1. And then, the mixed acid was added to MWNTs under sonication for 30 min, followed by heating at 80 °C for 1 h. In the next step, the suspension was washed with deionized water and dried under vacuum at 60 °C, so as to obtain functional MWNTs. A series of PVA/MWNT spinning dopes with R of MWNTs to PVA ranging from 0 to 5/95, 10/90 and 20/80 were produced. In a typical procedure for preparing PVA/MWNT composite fibers, 1 g PVA chips was dissolved in 30 ml deionized water under continuously stirring at 90 °C for 4 h. Meanwhile, the corresponding loading of functional MWNTs was dispersed in 40 ml deionized water and sonicated for 4 h. Then the functional MWNTs aqueous dispersion was added to the PVA aqueous solution and stirred at 90 °C overnight, and a 15 wt% water-soluble PVA/MWNT (hereafter referred to as functional MWNTs without special illustration) spinning dope could be obtained by concentrating.

2.3. Wet-spinning of continuous PVA/MWNT fibers

The water-soluble PVA/MWNT spinning dope was loaded into a 5 ml disposable syringe installed in a syringe pump, which was continuously injected into a methanol coagulation bath through a 21-gauge stainless needle with a 2.5 cm tube in length. Besides, the dope injection rate and the coagulating bath channel length were 3.0 ml/h and 1.2 m, respectively. After passing through the coagulation bath, the fiber was taken up and finally collected on scroll, and then dried under vacuum at 50 °C to remove methanol and water. Afterwards, continuous hot-drawing was performed on as-spun fibers at 140 °C with a draw ratio of 8, and as-spun fibers were hereafter denoted as PVA fiber. PVA/MWNT-1, PVA/MWNT-2 and PVA/MWNT-3 mean the composite fibers with 5 wt%, 10 wt% and 20 wt% MWNTs, respectively.

3. Measurements

Fourier transform infrared spectrum (FT-IR) in the range of 400-4000 cm^{-1} was obtained by a Nicolet 8700 Fourier transform infrared spectrometer (Thermo Electron, American) with KBr pellets of MWNTs, and under the averaging of 32 scans at a resolution of 4 cm^{-1}. With the help of a NETZSCH TG 209 F1 Analyzer, the content of MWNTs in composite fibers was investigated by means of thermogravimetric analysis (TGA) under nitrogen with a heating rate of 20 °C/min. Through a model XQ-1 tensile tester, tensile measurement was carried out at room temperature with a gauge length of 20 mm and crosshead speed of 20 mm min^{-1}. Operating at 10 kV, SEM images were acquired on a Philips-FEI Quanta 200 instrument. In addition, the differential scanning calorimetry (DSC) was conducted by employing a NETZSCH STA-409PC instrument and wide angle X-ray diffraction (WAXD) was implemented by adopting a Bruker AXS D8 Discover equipped with Cu Kα radiation (40 kV, 40 mA).

4. Results and discussion

As shown in Fig. 1, FTIR spectra of pristine and functional MWNTs were presented. Some similar characteristic peaks were found in both pristine and functional MWNTs. A stretching vibration band of O–H at about 3432 cm^{-1} maybe attributed to isolated O–H moieties and/or O–H in COOH groups and absorbed water [14]. The bands at 2973 cm^{-1}, 2923 cm^{-1} and 2854 cm^{-1} were corresponding to asymmetric stretching vibration band of CH_3, asymmetric and symmetric stretching vibration bands of CH_2, respectively [15]. The band at 1633 cm^{-1} was attributed to the C=C stretching vibration in graphitic layers [16,17]. However, functional MWNTs had some extra stronger peaks in their FTIR spectra. The strong band at 1733 cm^{-1} is the characteristic peak of C=O in COOH groups. The band at 1396 cm^{-1} was attributed to the O–H bending vibration in COOH groups [18]. The bands at 1166 cm^{-1} and 1070 cm^{-1} were the stretching vibration of C–O in ether and alcohol, respectively [15]. These results indicated that a number of oxygen-containing groups were introduced into MWNTs by treating with mixed acid.

As mentioned in the experimental procedure, pristine MWNTs and as-prepared functional MWNTs were dispersed in deionized water with a concentration of 0.5 mg mL^{-1} with the aid of ultrasonication. In the next step, dispersions were allowed to settle for a week. In Fig. 2, digital pictures of all the dispersions were collected immediately after sonication (A), 2 h after sonication (B) and a week after sonication (C). It could be noticed that even after a long time of ultrasonication (Fig. 2A), pristine MWNTs were not able to form stable suspensions in water, which gradually led to strong aggregation after settling for 2 h (Fig. 2B). A week later, pristine MWNTs eventually precipitated completely. On the contrary, suspensions of functional MWNTs were still highly stable even after settling for a week (Fig. 2C). It is noted that functional MWNTs could dispersed homogeneously in aqueous solution after the treatment of mixed acid. And good stabilization of functional MWNTs in water-soluble spinning dope is crucial to fabricating composite fibers.

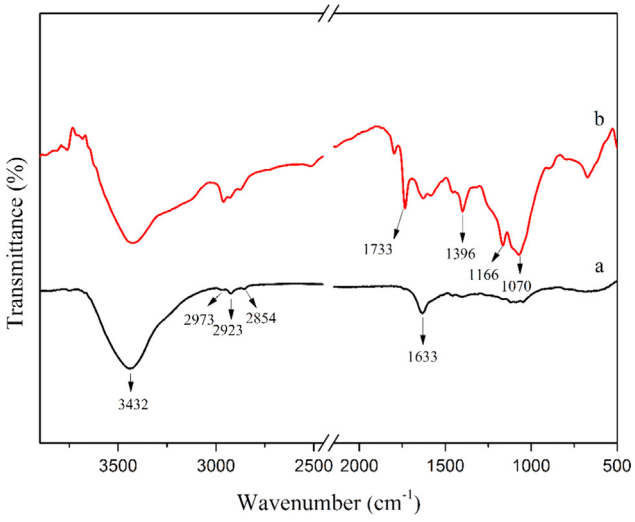

Fig. 1. FTIR spectra of (a) pristine MWNTs and (b) functional MWNTs.

Fig. 3 exhibited TG and several differential TG (DTG) curves of functional MWNTs, PVA fiber and PVA/MWNT-1, 2, 3 composite fibers (the *R* of MWNTs to PVA was 5/95, 10/90 and 20/80). For functional MWNTs, obvious weight loss was observed within a temperature range of 30–600 °C, which was caused by carboxyl, hydroxyl group and some amorphous carbons decomposition [19,20]. For PVA fiber, two distinct weight loss peaks were observed at around 380 and 450 °C, which were identified as the decomposition temperature of side chain and main chain of PVA, respectively. For composite fibers, the weight loss of both functional MWNTs and PVA were detected according to the observation in the DTA curve of composite fibers (i.e. PVA/MWNT-3 in Fig. 3e′). By virtue of the law of conservation of mass [12], TGA was frequently used to weigh the amount of MWNTs in the composite fibers. In order to calculate the content of MWNTs in composite fibers (C_{MWNT}), the following equation (Eq. (1)) was chosen:

$$C_{MWNT} = \frac{R_C - R_{PVA}}{R_{MWNT} - R_{PVA}} \times 100\% \quad (1)$$

Of which, R_{PVA}, R_{MWNT} and R_c represented the residual weight of PVA, MWNTs and PVA/MWNT composite fibers at 600 °C, respectively. The values of corresponding MWNTs content in composite fibers were listed in Table 1.

Typical stress–strain curve and average mechanical properties of PVA and PVA/MWNT drawn fibers were shown in

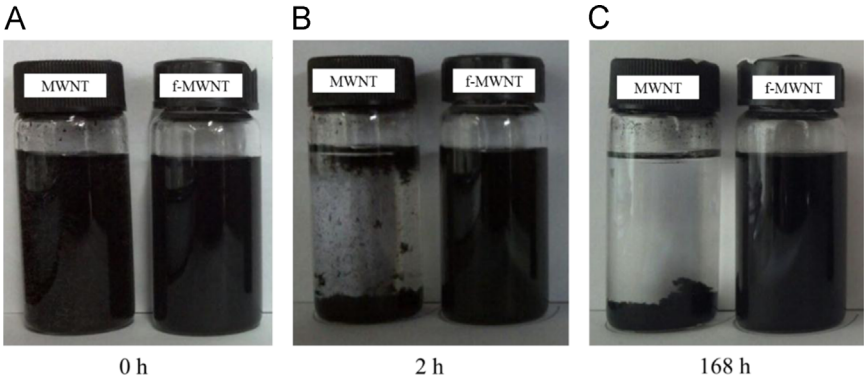

Fig. 2. Digital pictures of pristine and functional MWNTs dispersed in water through bath ultrasonication (0.5 h): (A) dispersions immediately after sonication, (B) dispersions 2 h after sonication, and (C) dispersions a week after sonication.

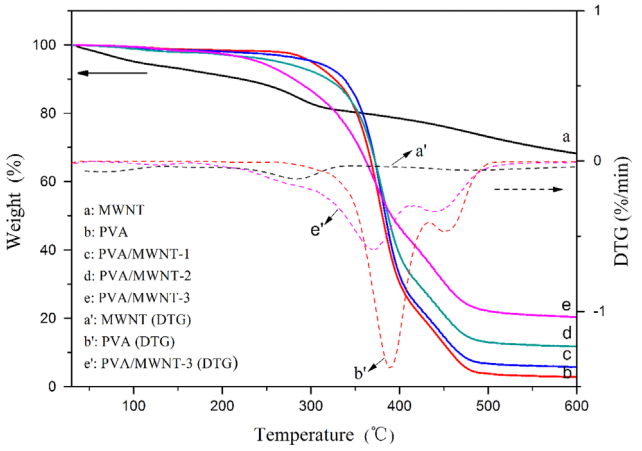

Fig. 3. TG curves of (a) functional MWNTs, (b) PVA fiber, and (c–e) PVA/MWNT composite fibers and some DTG curves of (a′) functional MWNTs, (b′) PVA fiber, (e′) PVA/MWNT-3.

Table 1
MWNTs content in composite fibers.

Sample	Feeding capacity of MWNTs (wt%)	Residual weight at 600 °C	MWNTs content in fibers (wt%)
PVA	0	2.2	–
PVA/MWNT-1	5	5.7	5.30
PVA/MWNT-2	10	11.7	14.4
PVA/MWNT-3	20	20.4	27.6

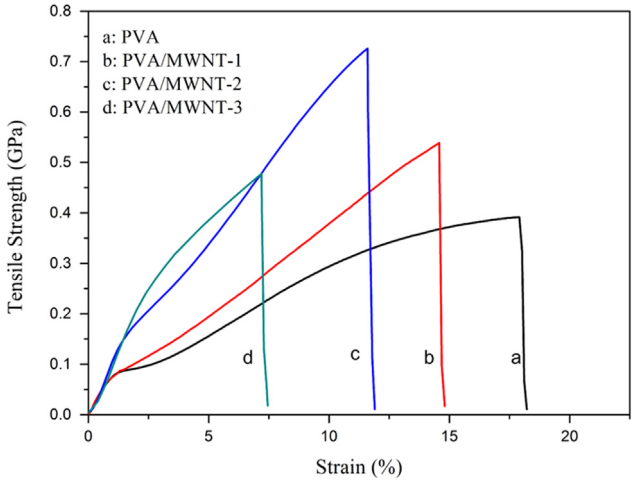

Fig. 4. Typical stress–strain curves of neat PVA and PVA/MWNT composite fibers.

Fig. 4 and Table 2. Compared with the pure PVA fiber, the curve of composite fibers exhibited a much steeper short initial slope, which indicated that Young's modulus of composites fibers was higher than that of the pure PVA fiber. With the increase of MWNTs content in the composite fibers, Young's modulus was significantly enhanced from 6.7 GPa for pure PVA fibers to 12.8 GPa for composite fibers with 27.6 wt% MWNTs. Furthermore, the tensile strength of composite fibers was significantly higher than that of the pure PVA fiber, and that of PVA/MWNT-2 composite fibers was almost twice as the PVA fiber. However, the tensile strength was declined dramatically as MWNTs (PVA/MWNT-3) increased continuously, which could be explained by the relationships between structure and properties, such as (1) poor dispersibilities of MWNTs [17], (2) weak interaction between polymer and MWNTs [21–23], (3) low orientation of MWNTs and PVA molecular chain [22,23]. Several characterization methods were employed to study the reason why the mechanical properties of composite fibers changed dramatically, such as SEM, DSC and WAXD.

Table 2
Mechanical properties of PVA fiber and PVA/MWNT composite fibers.

Sample	Diameter (μm)	Tensile strength (GPa)	Young's Modulus (GPa)	Elongation (%)
PVA	56.3	0.39	6.7	17.9
PVA/MWNT-1	43.3	0.53	7.8	14.6
PVA/MWNT-2	45.0	0.74	12.6	11.6
PVA/MWNT-3	58.9	0.49	12.8	7.9

Surface texture and cross section of PVA fiber and composite fibers were studied using SEM micrographs, as shown in Fig. 5. In Fig. 5 the fiber surface grooves were found to increase with an increase in MWNTs concentration, and the relatively smooth surface of PVA fiber was also found, however the numerous elongated grooves along the composite fiber surface were obvious. In order to investigate MWNTs dispersion in PVA matrix, SEM analysis at high magnification were carried out for cross section of the as-spun PVA fiber and composite fibers. As can be seen from Fig. 6(A–C), the cross section of PVA fiber was pure, while a number of small white dots representing MWNTs were found in composite fibers. In PVA/MWNT-1 and PVA/MWNT-2, MWNTs were homogeneously dispersed, which were not pulled out from PVA matrix in the wetting-off procedure. Good dispersibility of MWNTs in composite fibers is one of the significant reasons for high mechanical properties of composite fibers. But unfortunately, some agglomerates were observed in PVA/MWNT-3 (the cycle in Fig. 6(D)), which would have strong impact on the mechanical performance of composite fibers. The reason is that some voids/defects would generate between agglomerates and polymer matrix. For a common mechanical property testing, forces acting on voids would result in stress concentration under tensile loads, and hence the tensile strength of PVA/MWNT-3 was sharply declined.

As shown in Fig. 7, DSC measurements were adopted to characterize the interaction between MWNTs and PVA. Compared with the curves of composites fibers, a higher and narrower melting and crystallization peaks of neat PVA fiber were observed. As the content of carbon nanotubes increased,

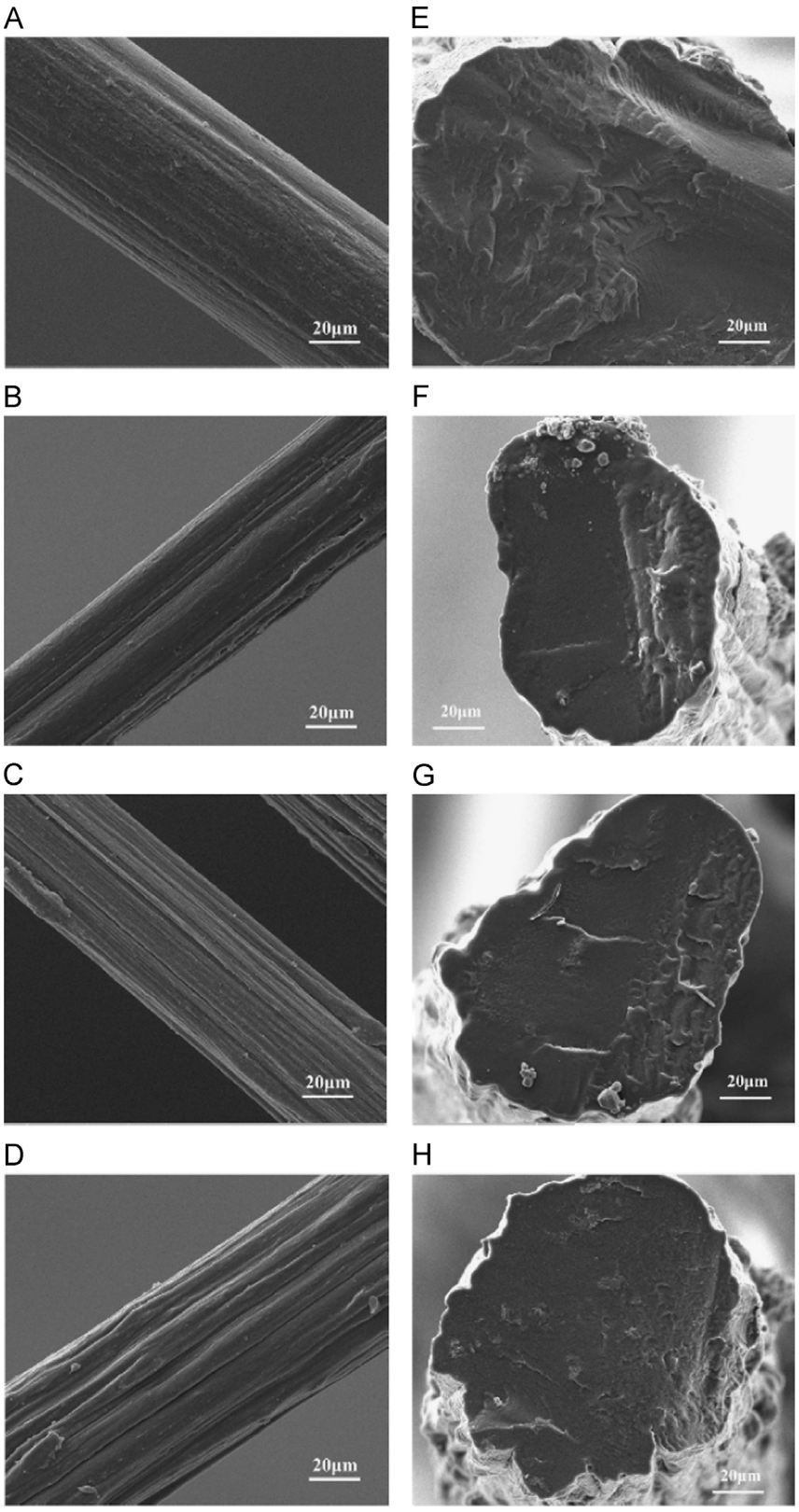

Fig. 5. SEM micrographs of the surface texture of drawn fiber and the cross section of as-spun fibers at low magnification: (A, E) PVA fiber, (B, F) PVA/MWNT-1, (C, G) PVA/MWNT-2 and (D, H) PVA/MWNT-3. Scale bar=20 μm.

these two peaks became wider and moved toward lower temperature, particularly the peaks for PVA/MWNT-3 containing 27.6 wt% MWNTs, which was almost vanished. That was to say, the area of melting and crystallization peaks was decreased with the increasing of MWNTs content, as was the case with crystallization temperature (T_c) and melting

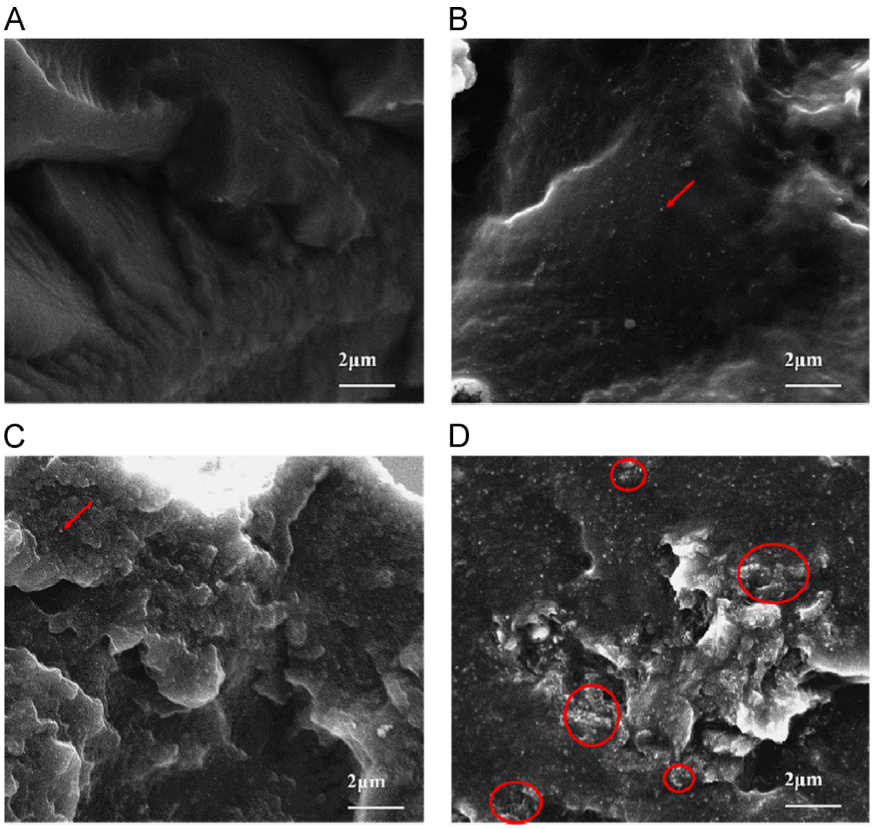

Fig. 6. SEM micrographs of the cross section of as-spun fibers at high magnification: (A) PVA fiber, (B) PVA/MWNT-1, (C) PVA/MWNT-2 and (D) PVA/MWNT-3. Scale bar=2 μm.

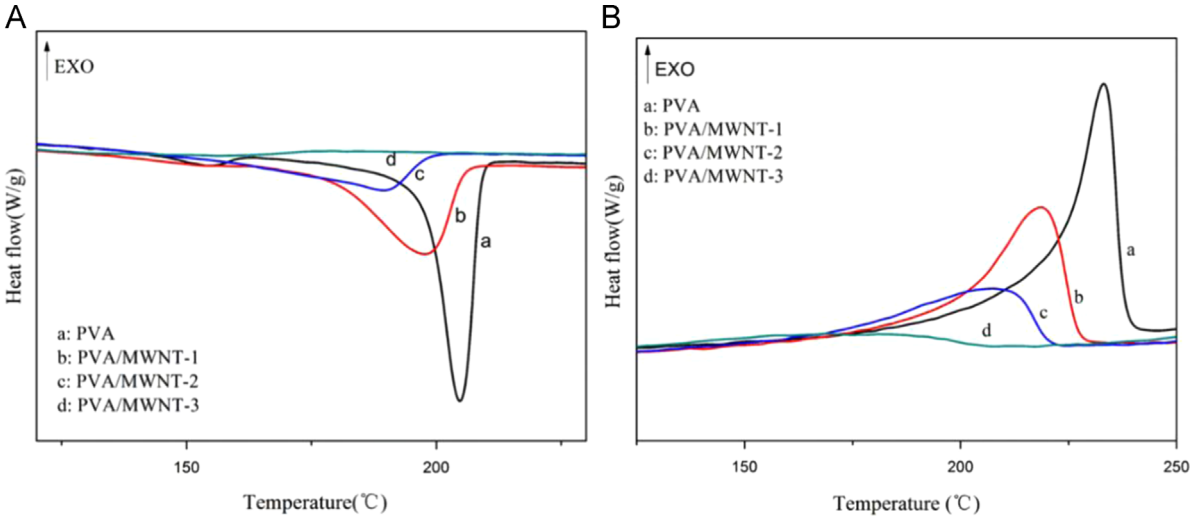

Fig. 7. DSC melt curves (A) and crystallization curve (B) of the PVA fiber and PVA/MWNT composite fibers.

temperature (T_m). These phenomenon were generated by the decline of the locomotivity of polymer chain. Due to the strong hydrogen bonding between the oxygen-containing groups of MWNTs and the PVA molecular chain [24], the motion of PVA chain was confined by MWNTs in the composite fibers. Furthermore, the strong interfacial interaction benefited composite fibers in efficient stress-transfer in composites, and this was one of the reasons that gave rise to the increase of the mechanical properties.

When X-rays were irradiated to isotropic samples, uniform diffraction rings occurred in WAXD patterns. Conversely, uneven diffraction rings appeared on the condition that X-rays were irradiated to anisotropic samples. As shown in Fig. 8(A–D), 2D WAXD patterns of the drawn PVA fiber and composite

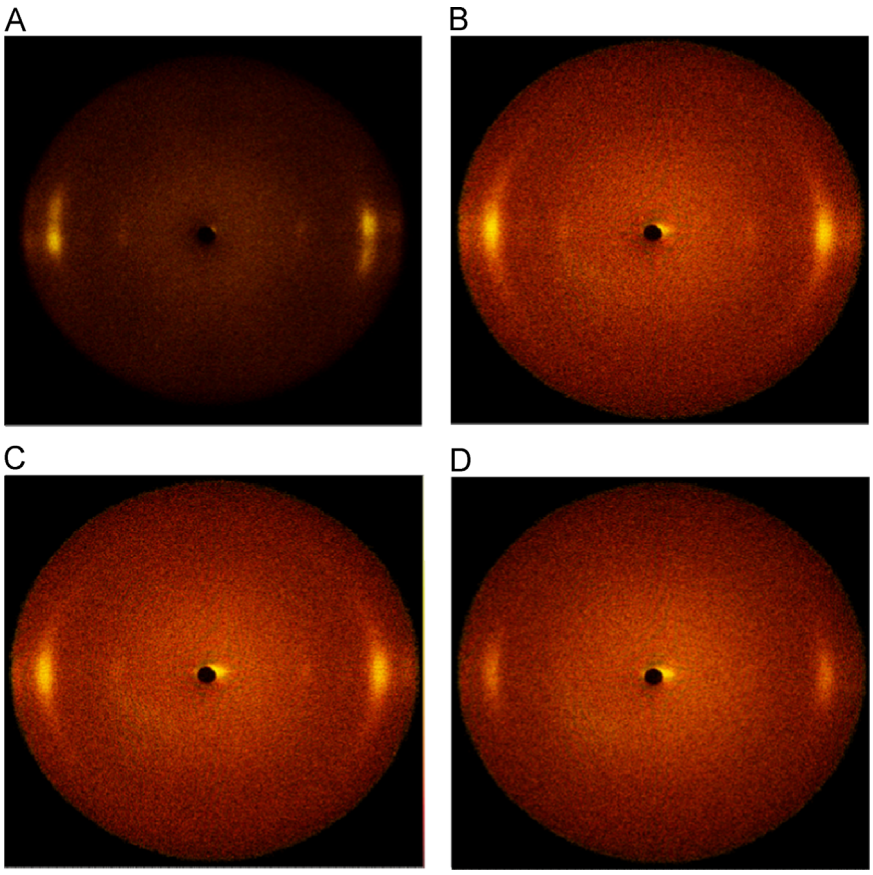

Fig. 8. Wide-angle X-ray patterns of (A) PVA fiber, (B) PVA/MWNT-1, (C) PVA/MWNT-2 and (D) PVA/MWNT-3.

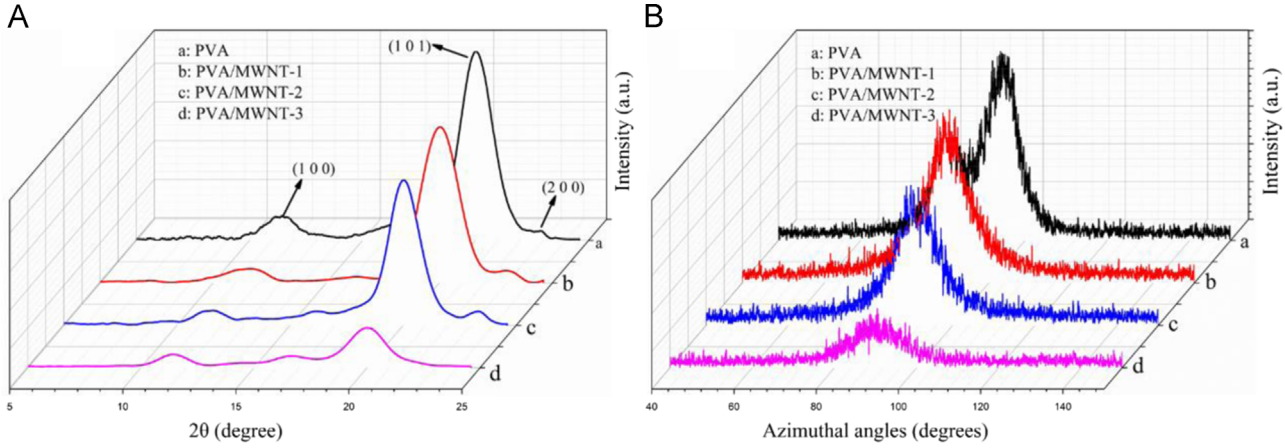

Fig. 9. (A) Integrated intensity curves along scattering angle at equator direction; (B) Integrated intensity curves of (101) along azimuthal angle.

Table 3
The degree of orientation of PVA molecules in PVA fiber and composite fibers.

Sample	D.O. (%)
PVA	94.1
PVA/MWNT-1	93.3
PVA/MWNT-2	92.1
PVA/MWNT-3	90.9

fibers exhibited crescent-shaped uneven diffraction rings, which indicated that PVA molecules were well-oriented. Along scattering angle at equator direction of the PVA fiber and composite fibers, integrated intensity of patterns was shown in Fig. 9A. In the spectrum, diffraction peaks at $2\theta = 11.5^\circ$, 20° and 23° were identified being attributed to the crystal face of (100), (101) and (200) [17], respectively. As shown in Fig. 9B, azimuthal scans of the peak at $2\theta = 20^\circ$ in Fig. 8 were obtained, so as to further explore the orientation of

PVA molecules in fibers. As shown in Table 3, the degree of orientation (D.O.) of PVA molecules in these fibers was calculated by using the Eq. (2) [25].

$$\text{D.O.} = \frac{180^\circ - \text{FWHM}}{180^\circ} \times 100\% \quad (2)$$

Of which, FWHM was the full-wide-at-half-maximum of azimuthal scans (Fig. 9(B)) of the peak at $2\theta = 20^\circ$. It was necessary to point out that Eq. (2) was an empirical formula, which had no obvious physical meaning. Nevertheless, it was beneficial to relative magnitudes comparison. With the increasing of MWNTs content in composite fibers, the orientation of PVA molecules was declined from 94.1% to 90.9%. Typically, the higher the D.O., the better the mechanical properties are [25]. However, it is not the only reason for the composites. The interfacial interaction and dispersion of MWNTs in matrix are always significant determinants, which were characterized by SEM and DSC above.

5. Conclusions

(1) Environmental friendly PVA/MWNT composite fibers containing a large proportion of MWNTs up to 27.6 wt% were successfully fabricated by the wet-spinning process. (2) As the content of MWNTs increased, the mechanical properties of the PVA composite fibers enhanced significantly. The Young's modulus of composite fibers gradually increased to 12.8 GPa for the fiber with 27.6 wt% MWNTs. And, the tensile strength gradually increased to 0.74 GPa for the fiber with 14.4 wt% MWNTs. (3) The SEM results indicated that MWNTs of the PVA composite fibers dispersed well in PVA matrix, however some agglomerates also existed as the content of MWNTs reached to 27.6 wt%. Besides, the grooves in the PVA composite fibers surface were found to increase with an increase in MWNTs concentration. (4) The DSC results showed that the area of melting and crystallization peaks was decreased with the increasing of MWNTs content, as was the case with crystallization temperature (T_c) and melting temperature (T_m). (5) WXAD characterization showed that the orientation of PVA molecules was declined from 94.1% to 90.9% with the increase of MWNTs content.

In conclusion, a homogeneous dispersibility of MWNTs throughout PVA matrix and efficient stress-transfer between MWNTs and PVA matrix are in response for significant enhancement in mechanical properties.

Acknowledgment

We acknowledge the research center for analysis and measurement of Donghua University. This work is supported by Innovation Program of Shanghai Municipal Education Commission (13ZZ052) and Fundamental Research Program of Science and Technology Commission of Shanghai Municipality (13NM1401502).

References

[1] S. Iijima, Nature 354 (6348) (1991) 56–58.
[2] A.B. Dalton, S. Collins, E. Munoz, J.M. Razal, V.H. Ebron, J.P. Ferraris, J.N. Coleman, B.G. Kim, R.H. Baughman, Nature 423 (6941) (2003) 703.
[3] J.K.W. Sandler, J.E. Kirk, I.A. Kinloch, M.S.P. Shaffer, A.H. Windle, Polymer 44 (19) (2003) 5893–5899.
[4] J. Zhang, Q. Wang, L. Wang, A. Wang, Carbon 45 (9) (2007) 1917–1920.
[5] C.A. Dyke, J.M. Tour, J. Phys. Chem. A 108 (51) (2004) 11151–11159.
[6] G. Clave, S. Campidelli, Chem. Sci. 2 (10) (2011) 1887–1896.
[7] X.F. Zhang, T. Liu, T.V. Sreekumar, S. Kumar, V.C. Moore, R.H. Hauge, R.E. Smalley, Nano Lett. 3 (9) (2003) 1285–1288.
[8] X. Li, S.Y. Wong, W.C. Tjiu, B.P. Lyons, S.A. Oh, C. Bin He, Carbon 46 (5) (2008) 829–831.
[9] M. Moniruzzaman, K.I. Winey, Macromolecules 39 (16) (2006) 5194–5205.
[10] P. Potschke, H. Brunig, A. Janke, D. Fischer, D. Jehnichen, Polymer 46 (23) (2005) 10355–10363.
[11] K.A. Anand, T.S. Jose, U.S. Agarwal, T.V. Sreekumar, B. Banwari, R. Joseph, Int. J. Polym. Mater. 59 (6) (2010) 438–449.
[12] M.H. Jee, J.U. Choi, S.H. Park, Y.G. Jeong, D.H. Baik, Macromol. Res. 20 (6) (2012) 650–657.
[13] L. Suhrenbrock, G. Radtke, K. Knop, P. Kleinebudde, Int. J. Pharm. 412 (1–2) (2011) 28–36.
[14] L. Stobinski, B. Lesiak, L. Koever, J. Toth, S. Biniak, G. Trykowski, J. Judek, J. Alloy. Compd. 501 (1) (2010) 77–84.
[15] B. Scheibe, E. Borowiak-Palen, R.J. Kalenczuk, Mater. Charact. 61 (2) (2010) 185–191.
[16] H. Yu, Y. Jin, Z. Li, F. Peng, H. Wang, J. Solid State Chem. 181 (3) (2008) 432–438.
[17] C.F. Fu, L.X. Gu, J. Appl. Polym. Sci. 128 (2) (2013) 1044–1053.
[18] T. Szabo, O. Berkesi, P. Forgo, K. Josepovits, Y. Sanakis, D. Petridis, I. Dekany, Chem. Mater. 18 (11) (2006) 2740–2749.
[19] V. Datsyuk, M. Kalyva, K. Papagelis, J. Parthenios, D. Tasis, A. Siokou, I. Kallitsis, C. Galiotis, Carbon 46 (6) (2008) 833–840.
[20] J. Xu, M. Zhang, M. Nakamura, S. Iijima, M. Yudasaka, Appl. Phys. A – Mater. Sci. Process. 100 (2) (2010) 379–383.
[21] C.Y. Wei, Nano Lett. 6 (8) (2006) 1627–1631.
[22] M.L. Minus, H.G. Chae, S. Kumar, Macromol. Chem. Phys. 210 (21) (2009) 1799–1808.
[23] H.G. Chae, M.L. Minus, S. Kumar, Polymer 47 (10) (2006) 3494–3504.
[24] L. Kou, C. Gao, Nanoscale 5 (10) (2013) 4370–4378.
[25] X. Wang, S.Y. Park, K.H. Yoon, W.S. Lyoo, B.G. Min, Fiber Polym. 7 (4) (2006) 323–327.